

Electron Specimen Interaction In Low Voltage Electron Beam Lithography

Weidong Liu

July 1995

To better understand resist charging effect and the interaction between low energy electrons and specimen, we performed more experiments to measure secondary electron (SE) emission coefficient (C_{se}) for the resist film. The samples are $0.4\mu\text{m}$ thick SAL601 or PBS on Chromium on quartz. The results for SAL601 and PBS samples are similar, we only show the result for SAL601 in Fig. 1. At voltages below 3.5 kV, when most of the incident electrons don't have enough energy to penetrate the resist layer and the resist can be viewed as bulk material, our C_{se} results have similar values as the C_{se} results for many other polymers [1]. The C_{se} increases with decreasing voltage, and crosses over 1 at about 1 kV. Below 1 kV the currents became dynamic, and the C_{se} couldn't be obtained. Above 3.5 kV, the C_{se} first decreases slowly with increasing voltage, and then finally settled to a value about 0.2 at 10 kV and beyond. For bulk material we expect to see C_{se} keep decreasing, because as incident energy goes up few electrons are scattered back and less energy is deposited at the top part of the surface therefore generating fewer SEs. However in this case, at higher incident energies more electrons can penetrate the resist layer and reach the substrate. The SE current measured is not only due to the SEs from the resist layer, but should also include the backscattered electrons from the substrate.

August 1995

In order to understand the charging mechanism better and quantitatively explain our experimental results, we simulated the electron interaction with the sample materials using Monte Carlo method. The model we used for electron scattering process was developed by R. Browning et al [2]. We simulated 100,000 electrons incident normally on the sample structure composed of $0.4\mu\text{m}$ resist on 80 nm Chromium on Quartz substrate, for the incident energy ranging from 1 keV to 20 keV. The results for SAL601 and PBS resist are very similar, and only the results for SAL601 are shown in Fig. 2 & 3. Fig. 2 is the fractions of electrons that backscattered from the sample (C_{bs}) and that trapped in the resist layer. Fig. 3 is the electron endpoint distribution.

The effect due to substrate scattering at different electron energies is evident in these figures. Below 3.5 keV, very few electrons can penetrate the resist layer so the sample behaves like bulk material (Fig. 3). In this range, C_{bs} decreases with the increasing energy, and the number of trapped electrons increases gradually (Fig. 2). As the energy goes above 3.5 keV, more electrons can penetrate resist film and interact with Chromium layer and substrate. We see the fraction of trapped electrons drops rapidly from about 90% at 3 keV to about 10% at 10 keV. C_{bs} becomes increasing slowly from 5 keV to 7 keV. This is because the substrate material's atomic number is higher than the average value of resist so there are more large angle scattering events. Above 7 keV most of the electron workpiece interaction takes place in the Quartz substrate, C_{bs} is about 0.13 although it decreases with energy very slowly.

September 1995

We repeated the measurement on electron beam induced conductivity (EBIC) in the resist film, and got the same result as reported before. In this experiment, a layer of 20nm Au/Pb was sputtered on top of our original sample, then 20V DC bias was applied across

DISTRIBUTION STATEMENT B
Approved for public release
Distribution Unlimted

DISTRIBUTION STATEMENT B

19970716 141



DEPARTMENT OF THE NAVY
OFFICE OF NAVAL RESEARCH
SEATTLE REGIONAL OFFICE
1107 NE 45TH STREET, SUITE 350
SEATTLE WA 98105-4631

IN REPLY REFER TO:

4330

ONR 247

11 Jul 97

From: Director, Office of Naval Research, Seattle Regional Office, 1107 NE 45th St., Suite 350,
Seattle, WA 98105

To: Defense Technical Center, Attn: P. Mawby, 8725 John J. Kingman Rd., Suite 0944,
Ft. Belvoir, VA 22060-6218

Subj: RETURNED GRANTEE/CONTRACTOR TECHNICAL REPORTS

1. This confirms our conversations of 27 Feb 97 and 11 Jul 97. Enclosed are a number of technical reports which were returned to our agency for lack of clear distribution availability statement. This confirms that all reports are unclassified and are "APPROVED FOR PUBLIC RELEASE" with no restrictions.
2. Please contact me if you require additional information. My e-mail is *silverr@onr.navy.mil* and my phone is (206) 625-3196.

Robert J. Silverman
ROBERT J. SILVERMAN

the resist film during electron irradiation. Beam induced current was a small fraction of the primary current, and it increases as the electron energy is lowered. This means at steady state the charge rearrangement effect is insufficient to eliminate the surface potential.

Then the positive surface potential observed at higher beam energy and thinner resist [3] can be explained as the following. The surface potential results from two populations of charges, the negative charge of trapped primary electrons in the resist film and its image charges, and the positive charge due to secondary electrons escaping from the top 10-20 nm (estimated 'escape depth'). In thinner resists or with higher primary energies a greater fraction of the primary electrons reaches the conducting substrate thus leaving a smaller fraction trapped in the resist film. Therefore the first component becomes smaller, and the net surface potential can be positive. Using our results at 10 keV, we see the secondary electron emission coefficient (C_{se}) is about 0.21 (Fig. 1) and the fraction of backscattered incident electrons (C_{bs}) only accounted for 0.13 of it (Fig. 2). The rest of the electrons coming out of the surface must be the secondary charges generated by either the primary electrons or the backscattered electrons in the resist. When they escape, there should be equal amount of positive charges left in the resist. Although the amount (0.08 of total incident electrons) is about the same as the trapped primary charges (~0.08 in Fig. 2), the positive charges have positions closer to the surface than the trapped electrons. Therefore the surface potential should be positive (even taking into account the image charges due to the conductive substrate). As the energy becomes larger than 10 keV, C_{se} and C_{bs} (Fig. 1&2) change very slowly, while the trapped electron becomes even fewer and closer to the substrate (Fig. 2&3). So we should expect to see a slowly increasing positive surface potential with increasing primary energy, consistent with our earlier experiment result.

We are developing a model to simulate secondary electron generation and emission for resist materials. This will allow us to use Monte Carlo simulation and C_{se} measurement data to quantitatively predict resist charging under a wide range of exposure conditions.

October 1995

Miniature low voltage electron beam system with compact SE detector

Our objective in this new project is to design and test a miniature electron beam column which has small probe size and low landing energy and a compact secondary electron detector that can be incorporated inside the micro-column for microscopy applications. In our current design, the objective lens comprises a micro-einzel lens followed by a retarding electrode just upstream of the sample, see Fig. 4. The testing setup is shown in the same figure. The electrodes were made of stainless steel sheets and the spacers are ceramic sheets. Primary electron optics simulation results show that the retarding aperture thickness is critical to the beam aberrations.

- 1 R. Browning and R. F. Pease et al, J. Appl. Phys. 76(4), 2016 (1994).
- 2 D. C. Joy and S. Lou, Scanning 11, 176 (1989).
- 3 W. Liu, J. Ingino, and R. F. Pease, J. Vac. Sci. Technol. B 13(5), (1995).

DTIC QUALITY INSPECTED 2

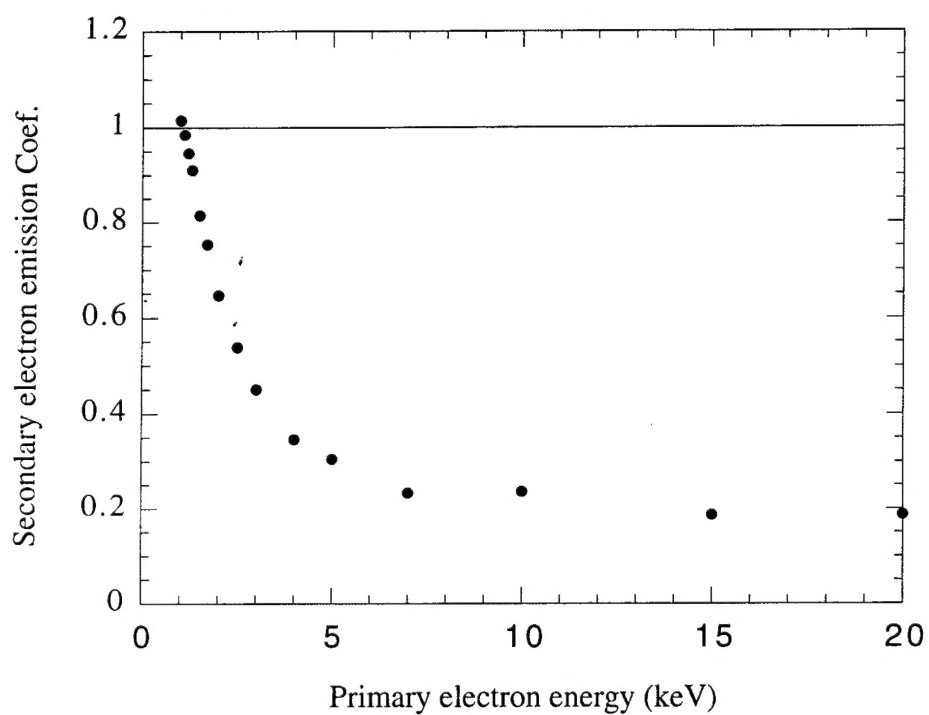


Fig. 1. Second electron emission coefficient.
The sample is SAL601 $0.4\mu\text{m}$ thin resist on Cr on quartz.

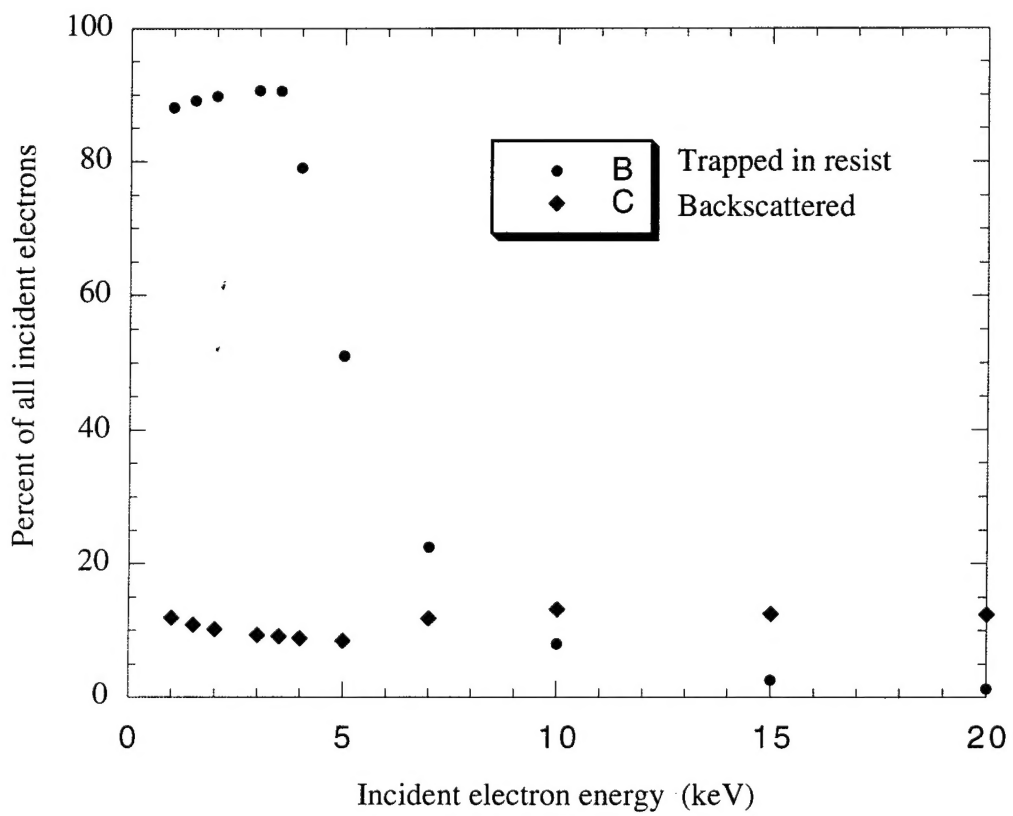


Fig. 2. Monte Carlo simulation of electrons backscattered and trapped in resist.
The sample is $0.4\mu\text{m}$ resist on 80nm Cr on quartz substrate.

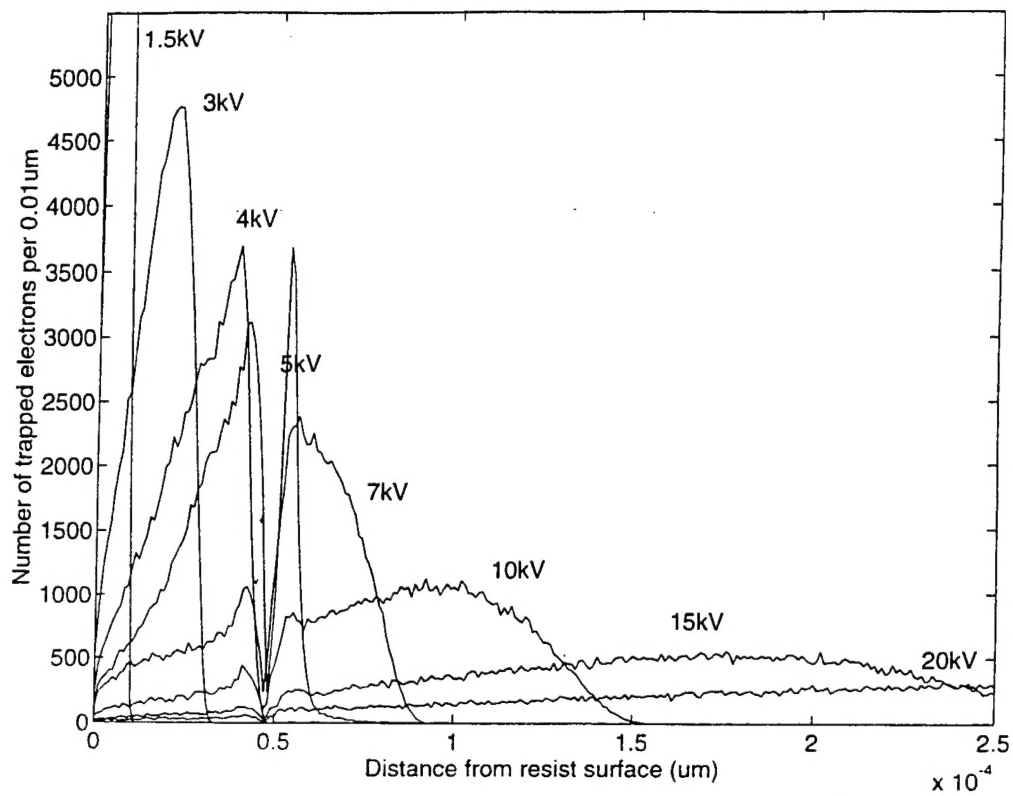


Fig. 3. Monte Carlo simulation of electrons endpoint distribution in resist.
The sample is 0.4 μm SAL601 on Cr on quartz substrate

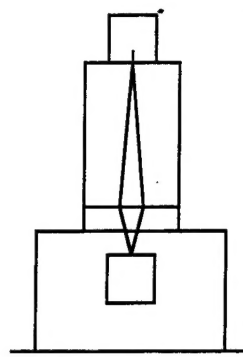


Fig. 4. Miniature electron optics system testing arrangement

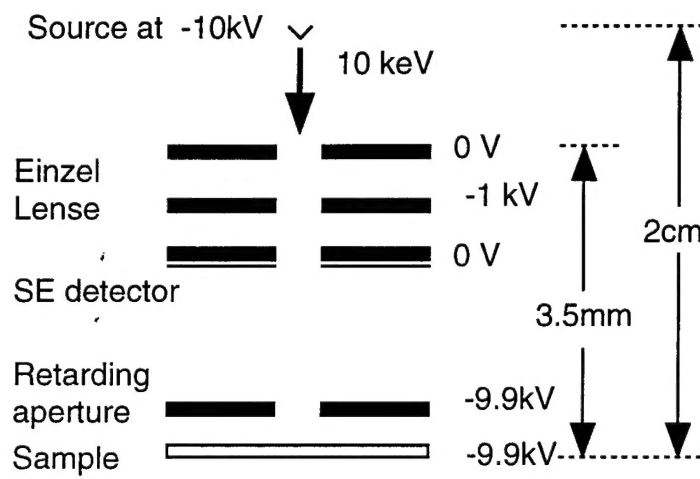


Fig. 4. Objective lens of miniature electron beam system

Monthly Reports for ARPA

James E. Schneider

July:

The bulk of the month was spent in design work for the ultrahigh vacuum (UHV) multi-purpose activation chamber, electron gun, and analysis chamber for the investigation of negative electron affinity (NEA) photocathodes. A great deal of effort was devoted to planning and general design work necessary to make the proposed equipment versatile. The analysis chamber reached its final design stage, and the design was sent out to be machined. Additional conceptual design took place for the activation chamber. The SPIE conference took place this month, during which the first disclosure of the results of the sealed-tube cathode work was made.

August:

A significant portion of the month was devoted to understanding activation procedures reported in the literature in preparation for the design of the activation chamber. In the middle part of the month, the activation chamber design was finished and sent out to be machined. Time was also spent in tasks relating to ordering of necessary equipment, and specifying a number of custom pieces of equipment necessary for the project. In particular, the custom light optics equipment was designed in accordance with the concept of small emission spot size through diffraction limited imaging.

September:

Further work was done in the design of other parts of the UHV system, including the electron gun itself, the load lock, and the UHV manipulation stages necessary in order to integrate the system. The differential pumping scheme for the electron optics column was finalized, as was the basic structure of the electron optics. Additional time was spent in understanding more detailed theoretical aspects of negative electron affinity itself. The submitted abstract for the 1995 IEEE Electron Devices Meeting was accepted.

October:

The final design for the bulk of the UHV system was frozen, and the remaining necessary equipment was purchased. Some time was spent in the testing and evaluation of equipment already received, in anticipation of the arrival of critical system components in November. Electron optics simulations of the proposed design alternatives for the electron beam column were begun.

Aaron Baum -- Negative Electron Affinity Photocathodes

July 1995

Design of photocathode activation chamber, electron gun, electron beam analysis chamber. Ordering parts for system. Repeated some of previous brightness measurements on new Mark III tube.

August 1995

Continued design and ordering of parts for demountable electron gun system. Preliminary construction of some parts. Set up lab area for new apparatus.

Submitted abstract to IEDM 1995 conference concerning computer cathode simulation work. Completed work on simulation.

September 1995

Continued design and ordering of parts for demountable electron gun system. Custom part designs sent to machine shop. Preliminary construction of some parts.

October 1995

Activation chamber arrives; actual construction begins. Designing, machining, and ordering continues.